

# Time-dependent Calculations of Electron Energy Distribution Functions for Cold Argon Gas in the Presence of Intense Black-Body Radiation

Joseph Abdallah Jr., James P. Colgan, T-1

Fig. 1. The black-body radiation field ( $\text{cm}^{-3} \text{eV}^3$ ) for radiation temperatures of 100, 200, and 300 eV.

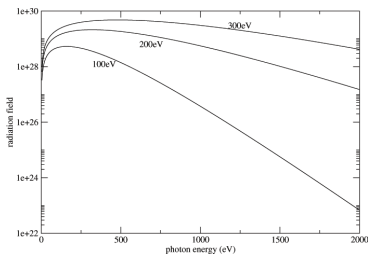
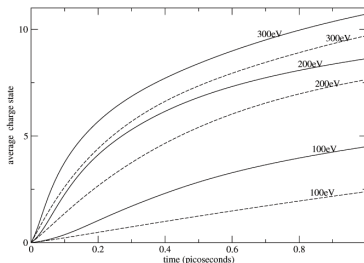


Fig. 2. The calculated average charge state ( $Z^*$ ) as a function of time (picoseconds) for radiation temperatures of 100, 200, and 300 eV. The solid lines are the results of the full model while the dashed lines correspond to calculations where collisional excitation and ionization have been neglected.



Boltzmann electron kinetic simulations are performed to study the time development of the electron energy distribution in a plasma that results from a cold argon gas subject to a black-body radiation source (100–300 eV). The study provides insight into the role of ionized electrons on the kinetics during a period of irradiation. The simulations are performed without any assumptions of electron temperature. The distributions are calculated as a function of time through 1 ps using Boltzmann kinetics, including the appropriate processes that alter state populations and electron energy. The processes included in the electron and atomic kinetics are collisional excitation/de-excitation, photo-excitation/decay, photo-ionization/radiative-recombination, collisional ionization, and auto-ionization/di-electronic capture. In addition, terms are included in the electron kinetics to account for electron-electron interactions and for free-free radiation absorption and emission. Results are presented that follow the evolution of the ionization state effective temperature as well as the electron energy distribution function (EEDF). The role of inelastic electron collisions, photo-ionization, auto-ionization, resonant radiative excitation, and electron-electron interactions are discussed.

High-energy density physics devices such as the Z pinch [1,2] have been used to create astrophysical laboratory plasmas by irradiation of matter with an intense source of X-rays. The emerging X-ray free electron laser (XFEL) [3] technology also has many interesting applications involving laser-matter interactions (for example, [4]). The Z pinch is capable of generating black-body radiation of several hundred eV, while XFEL produces a monochromatic X-ray source at tunable wavelengths. Each is capable of providing radiation capable of exciting and ionizing outer- and inner-shell electrons of atoms through direct and Auger processes. The free electrons then form a plasma whose properties are defined by their electron energy distribution function (EEDF). Both photon and electron processes occur to varying degrees after the initial plasma is formed while the radiation source is active. Spectroscopic properties of plasmas can be very sensitive [5-7] to the EEDF, especially the high-energy behavior.

This paper presents proof of principle simulations of the plasma EEDF, up to 1 ps, when argon gas is irradiated by black-body (100-300 eV) radiation, and provides insight about the important processes occurring in the plasma under these conditions. Unfortunately, there are no measurements of the EEDF for comparison purposes. The authors are unaware of any similar calculations under these conditions. The approach used is an extension of previous calculations [8,9] used to model the X-ray spectra resulting from the interaction of a high-power ultra-fast laser with argon clusters. In the latter work, an EEDF calculated from a particle in cell (PIC) code was used as an initial

condition. This EEDF was propagated in time by the simultaneous solution of atomic rate equations and Boltzmann electron kinetics. The atomic kinetics keeps track of atomic state populations while the electron kinetics keeps track of the distribution of electron energy. The two, are coupled to each other. Electron impact collisional excitation, de-excitation, ionization, and electron-electron collisions were used in the electron kinetics.

We start out with cold neutral argon gas and follow the EEDF directly, again using both atomic and electron kinetics. The electron kinetics capability was enhanced for this problem. Photo-ionization, radiative recombination, auto-ionization, di-electronic capture and free-free absorption and emission were incorporated in the electron kinetics package. A reduced detailed configuration accounting (RDCA) atomic model [10,11] was used. RDCA is an average of more detailed atomic models designed to be much faster while approximately preserving the atomic kinetics.

For the model calculations considered here, the atom number density was taken to be  $1 \times 10^{20} \text{ cm}^{-3}$ , and initially all the ions were assumed to be in the ground state of the neutral argon. One hundred time intervals between 0 and 1 ps were chosen and the scheme described above was used to obtain the EEDF and state populations as a function of time. The external radiation field  $G(h\nu)$  remained constant for the entire time period and temperatures of 100 eV, 200 eV and 300 eV were used in the simulations. The radiation field corresponding to these temperatures

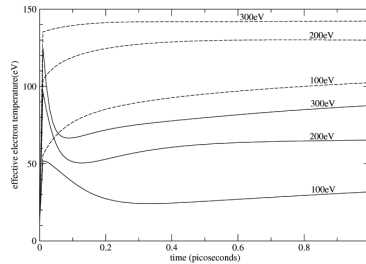


Fig. 3. The calculated effective temperature ( $kT^*$ ) in eV as a function of time (picoseconds) for radiation temperatures of 100, 200, and 300 eV. The solid lines are the results for the full calculation while the dashed lines correspond to calculations where collisional excitation and ionization have been neglected.

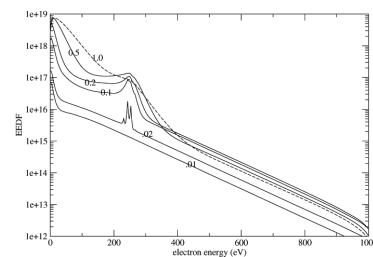


Fig. 4. The calculated electron energy distribution function (EEDF) in  $\text{cm}^{-3} \text{eV}^{-1}$  as a function of electron energy for 0.01, 0.02, 0.1, 0.2, 0.5, and 1.0 ps during irradiation by a 100-eV black-body radiation field.

is shown in Fig. 1. The EEDF was divided into 500 equally spaced bins from 0 to 1 KeV. The average charge state ( $Z^*$ ) and effective temperature ( $kT^*$ ) of electrons are calculated from the EEDF as a function of time. Note that after the time and energy grids have been carefully chosen, the only input to the model is the initial conditions and the radiation temperature.

The average charge state ( $Z^*$ ) is plotted (solid curves) as a function of time for radiation temperatures of 100, 200, and 300 eV in Fig. 2. Note that the degree of ionization increases with increasing temperature. For 200 and 300 eV, the ionization increases rapidly at first and then levels out, while the ionization is much slower at 100 eV. The predicted  $Z^*$  at 1 ps is 4.5, 8.6, and 10.7 for 100, 200, and 300 eV, respectively.

Figure 3 shows the calculated effective electron temperatures as a function of time for the same three cases. Each case shows an initial rapid heating of electrons, followed by rapid cooling until about 0.2 ps, and then slow heating. The initial rapid heating is caused by ionization in the neutral gas due to the radiation field. After sufficient free electrons are created, the plasma cools due to inelastic collisions of electrons with atoms and ions through excitation and ionization processes. The cooling occurs much faster at 300 eV than 100 eV because the higher rate of ionization results in a larger free electron density at 300 eV. After the plasma has cooled sufficiently, the electrons are then again slowly pumped by the radiation source. The dashed curves in Fig. 3 have been included in order to illustrate the effect of cooling. These curves correspond to the same radiation temperatures except that the effects of electron collisional excitation and ionization have been omitted. Here the effective temperature rises rapidly for each case and then levels off. This cooling effect at a radiation temperature of 300 eV accounts more than a 55-eV difference in the electron temperature.

It is interesting to compare the influence of ionization due to electrons versus the radiation field. The dashed curves in Fig. 2 correspond to calculations where collisional excitation and ionization have been neglected in both the electron and atomic kinetics. At a radiation temperature of 100 eV, about half the ionization is due to electrons. Note that as the temperature of the radiation field increases the role of the electrons diminishes as one would expect. At a radiation temperature of

300 eV and 1 ps the electrons account for a small yet significant amount of ionization, about one charge state in ten.

Figure 4 shows the calculated EEDF at various times for the 100 eV radiation temperature case. Note the EEDF does not assume a Maxwellian form over the entire time interval and electron energy range. At .01 ps the EEDF is formed by direct photo-ionization and has a tail (high energy part) that falls like its cross-section. The low photon energy behavior is produced by a combination of the peak of the photo-ionization cross-section and the electron-electron interaction, which tends to smooth and equilibrate the electron distribution. At .02 ps a bump appears at electron energies above 200 eV. This bump corresponds to the production of Auger electrons formed by inner shell excitations and ionizations from the  $n=2$  (L) shell of argon by the radiation field. Note that as time increases more free electrons are produced, the electron-electron interactions become stronger, and the bump gets smoother, but still persists even at 1 ps. At energies below 100 eV for later times, the Maxwellian shape takes form.

Note that EEDF calculations also include the production Auger electrons from K-shell excitation and ionization. However, K-shell vacancies have little effect on the results because fewer photons have energies in excess of 3000 eV, which is required for exciting such states. No K-shell bumps appear in the EEDF since they occur beyond the electron energy grid used here.

- [1] Mancini, R.C. et al., *Phys Plasma* **16**, 041001 (2009).
- [2] Hall I.M. et al., *Astrophys Space Sci* **322**, 117 (2009).
- [3] Pelliogrini, C., *Proc 16th Topical Conf Atomic Process Plasma*, 113 (2009).
- [4] Rosmej, F.B. et al., *High Energy Density Physics* **3**, 218 (2007).
- [5] Hansen, S.B. and A.S. Shlyaptseva, *Proc 14th Topical Conf Atomic Process Plasma*, 213 (2004).
- [6] Abdallah, J. Jr. et al., *J Quant Spectros Radiative Tran* **62**, 1 (1999).
- [7] Abdallah, J. Jr. et al., *Phys Scripta* **53**, 705 (1996).
- [8] Abdallah, J. Jr. et al., *Phys Rev A* **68**, 063201 (2003).
- [9] Sherrill, M.E. et al., *Phys Rev E* **73**, 066404 (2006).
- [10] Abdallah, J. Jr. and M.E. Sherrill, *High Energy Density Phys* **4**, 124 (2008).
- [11] Abdallah, J. Jr. et al., *High Energy Density Phys* **5**, 204 (2009).

#### Funding Acknowledgement

DOE, NNSA Advanced Simulation and Computing Program, Physics and Engineering Models